Distribution of Organohalide-Respiring Bacteria between Solid and Aqueous Phases

ARTICLE *in* ENVIRONMENTAL SCIENCE AND TECHNOLOGY · AUGUST 2014

Impact Factor: 5.33 · DOI: 10.1021/es501320h · Source: PubMed

6 AUTHORS, INCLUDING:

Carmen Lebron
Self Employed
44 PUBLICATIONS **489** CITATIONS
SEE PROFILE

Kurt D Pennell
Tufts University
171 PUBLICATIONS **3,472** CITATIONS
SEE PROFILE

Frank E Löffler
University of Tennessee
121 PUBLICATIONS **5,223** CITATIONS
SEE PROFILE

Environmental Science & Technology

Article

pubs.acs.org/est

Distribution of Organohalide-Respiring Bacteria between Solid and Aqueous Phases

Natalie L. Cápiro,*[,†] Yonggang Wang,[†] Janet K. Hatt,[‡] Carmen A. Lebrón,[§] Kurt D. Pennell,[†] and Frank E. Löffler*[,∥,⊥,#,∇]

[†]Department of Civil and Environmental Engineering, Tufts University, Medford, Massachusetts 02155, United States

[‡]School of Civil and Environmental Engineering, Georgia Institute of Technology, Atlanta, Georgia 30332, United States

[§]Naval Facilities Engineering Command, Engineering Service Center, Port Hueneme, California 93043, United States

[∥]Department of Microbiology, University of Tennessee, Knoxville, Tennessee 37996, United States

[⊥]Department of Civil and Environmental Engineering, University of Tennessee, Knoxville, Tennessee 37996, United States

[#]Center for Environmental Biotechnology, University of Tennessee, Knoxville, Tennessee 37996, United States

[∇]University of Tennessee and Oak Ridge National Laboratory (UT-ORNL) Joint Institute for Biological Sciences (JIBS) and Biosciences Division, Oak Ridge National Laboratory, Oak Ridge, Tennessee 37831, United States

Supporting Information

ABSTRACT: Contemporary microbial monitoring of aquifers relies on groundwater samples to enumerate nonattached cells of interest. One-dimensional column studies quantified the distribution of bacterial cells in solid and the aqueous phases as a function of microbial species, growth substrate availability and porous medium (i.e., Appling soil versus Federal Fine Ottawa sand with 0.75% and 0.01% [w/w] organic carbon, respectively). Without supplied growth substrates, effluent from columns inoculated with the tetrachloroethene- (PCE-) to-ethene-dechlorinating bacterial consortium BDI-SZ containing *Dehalococcoides mccartyi* (*Dhc*) strains and *Geobacter lovleyi* strain SZ (*Geo*SZ), or inoculated with *Anaeromyxobacter dehalogenans* strain W (*Adehal*W), captured 94−96, 81−99, and 73−84% of the *Dhc*, *Geo*SZ, and *Adehal*W cells, respectively. Cell retention was organism-specific and increased in the order *Dhc* < *Geo*SZ < *Adehal*W. When amended with 10 mM lactate and 0.11 mM PCE, aqueous samples accounted for 1.3−27 and 0.02−22% of the total *Dhc* and *Geo*SZ biomass, respectively. In Appling soil, up to three orders-of-magnitude more cells were associated with the solid phase, and attachment rate coefficients (k_{att}) were consistently greater compared to Federal Fine sand. Cell-solid interaction energies ranged from −2.5 to 787 *k*T and were consistent with organism-specific deposition behavior, where *Geo*SZ and *Adehal*W exhibited greater attachment than *Dhc* cells. The observed disparities in microbial cell distributions between the aqueous and solid phases imply that groundwater analysis can underestimate the total cell abundance in the aquifer by orders-of-magnitude under conditions of growth and in porous media with elevated organic carbon content. The implications of these findings for monitoring chlorinated solvent sites are discussed.

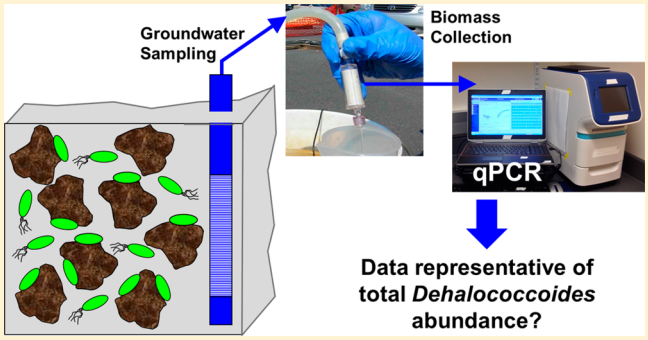

INTRODUCTION

The assessment of microbial populations in aquifers is primarily performed using groundwater samples due to the difficulties and costs associated with the collection of solid samples.[1] Cell abundances are reported per volume of groundwater (e.g., cells/L), and serve as indicators of the feasibility of monitored natural attention (MNA) and the success of enhanced bioremediation.[2−4] An added advantage of groundwater collection is that the sample integrates over a larger aquifer volume, thereby reducing the need to collect multiple solid samples to assess local heterogeneity.[3,5] The analysis assumes that the abundance of target microbial cells in groundwater represents, or at least correlates with, the total number of microbes of interest present in the aquifer formation.

A number of experimental studies suggest that the distribution of microbes between the solid and aqueous phases is not consistently uniform and is influenced by a variety of factors, including the physiological state of the organisms,[6] growth phase,[7,8] geochemical conditions (e.g., ionic strength, pH),[9] contaminant concentrations,[10−12] nutrient availability,[1]

Received: March 17, 2014
Revised: July 31, 2014
Accepted: August 6, 2014
Published: August 8, 2014

hydrodynamic shear forces,[13,14] and the properties of the aquifer matrix (e.g., permeability, surface charge).[1,9,15−19] Furthermore, microbial attachment is a species-specific, dynamic process.[1] Bacterial cells may attach to aquifer solids, with only a small fraction existing in a nonattached ("planktonic") state,[20−22] or exhibit negligible tendency to associate with the solids.[23−26] The environmental conditions and organismal properties determine what fraction of cells of the same population is associated with the solid and the aqueous phases.[16,18] For example, at uranium-contaminated sites, equal numbers of *Geobacter* spp. 16S rRNA genes were associated with solid and groundwater samples following biostimulation;[27−30] however, cells were predominately planktonic (up to 2 orders-of-magnitude higher than solid-attached cells) during Fe(III) reduction,[31] and were primarily associated with the solid phase during subsequent sulfate reduction.[31] In contrast, attached uranium-reducing *Anaeromyxobacter* cells outnumbered nonattached cells up to 4 orders-of-magnitude following biostimulation.[29]

Laboratory column experiments have demonstrated preferential attachment of *Geobacter lovleyi* strain SZ (*Geo*SZ) cells in the vicinity of a PCE source zone, whereas nonattached *Geo*SZ cells dominated the plume region.[11] Conversely, *Dehalococcoides mccartyi* (*Dhc*) cells attached throughout the source zone and plume regions within this column system.[11] In contrast, experiments evaluating dissolved-phase *cis*-1,2-dichloroethene (*cis*-DCE) and vinyl chloride degradation revealed negligible *Dhc* cell attachment to sandy clay.[26] Similarly, borehole samples from a trichloroethene- (TCE-) contaminated aquifer only detected *Dhc* cells in groundwater samples, but not in solid samples collected from the same location.[24] Despite the potential variability in the phase distribution of bacterial cells, conclusions of dechlorination performance are typically based on biomarker gene enumeration of groundwater samples. Measurement of 10^6 *Dhc* cells/L or greater in groundwater is used as an indicator for complete dechlorination of PCE/TCE to ethene and thus, guides management decisions at sites impacted by chlorinated solvents.[2,3,32,33]

The objective of this study was to develop a deeper understanding of the distribution of dechlorinating bacteria between the aqueous and solid phases, based on quantitative real-time PCR (qPCR) measurements. The phase distribution of three organohalide-respiring bacterial populations, *Dhc*,[34] *Geo*SZ,[35] and *Anaeromyxobacter dehalogenans* strain W (*Adehal*W),[29] was examined in a series of column experiments performed under nongrowth and growth conditions in two representative porous media, Federal Fine Ottawa sand and Appling soil. In addition, the surface characteristics of the cultures were measured and related to the extent of cell attachment to solids.

MATERIALS AND METHODS

Porous Media and Solution Preparation. Federal Fine Ottawa sand (30−140 mesh) with an organic carbon content of 0.1 mg/g, a mean grain size (d_{50}) of 0.32 mm and an intrinsic permeability of 4.2×10^{-11} m^2 was purchased from U.S. Silica Company (Berkeley Spring, WV).[36] Appling soil with 7.5 mg/g organic carbon content, a d_{50} of 0.22 mm, an intrinsic permeability of 1.2×10^{-11} m^2,[37] and a particle size distribution of approximately 77% sand, 14% silt, and 9% clay size fractions[38] was obtained from the University of Georgia Agricultural Experiment Station (Eastville, GA).

Mineral salts medium with an ionic strength of approximately 60 mM buffered to a pH of 7.2 ± 0.2 with potassium phosphate and reduced with 0.2 mM Na_2S was prepared as described.[11,39,40] Where indicated, the medium was amended with 10 mM sodium lactate as electron donor and PCE (0.11 mM, aqueous phase) (HPLC-grade, 99.5% purity; Fisher Scientific, Fair Lawn, NJ). Aqueous solutions containing sodium bromide (6,173 mg/L, Fisher Scientific) as a conservative tracer and calcium chloride (2220 mg/L, Fisher Scientific) as a background electrolyte were prepared in deionized, degassed water (Nanopure; Barnstead/Thermolyne Corp., Dubuque, IA).

Bacterial Cultures. The nonmethanogenic, PCE-to-ethene-dechlorinating consortium, Bio-Dechlor INOCULUM (BDI-SZ), contains *Dhc* strains FL2, GT and BAV1, and *Geo*SZ.[11,39,41−43] The consortium was maintained with 0.33 mM PCE and 10 mM lactate. *Adehal*W was maintained in medium with 5 mM acetate (Sigma-Aldrich, St. Louis, MO) and 10 mM fumarate (Sigma-Aldrich) as the electron acceptor.[44] *Dhc* strain BAV1,[45] *Dhc* strain FL2,[46] *Dhc* strain GT,[40] and *Geo*SZ (DSM17278)[35] were maintained with chlorinated ethenes as electron acceptors as described.[35,40,45,46] Protocols for qPCR target gene and cell enumerations are described in the Supporting Information (SI).

Transport and Retention of Bacterial Cells Following Inoculum Delivery. The transport and retention characteristics of *Dhc* and *Geo*SZ cells, as well as *Adehal*W cells, were measured in borosilicate glass columns (2.5 cm diameter, 10 cm length; Kimble-Chase, Vineland, NJ) under up-flow operation. A nonreactive tracer solution, consisting of bromide dissolved in reduced mineral salts medium, was introduced at a flow rate of 1 mL/min to quantify the aqueous phase pore volume (PV) and assess flow conditions in each column. The porosity the Appling soil and Federal Fine sand columns ranged from 0.34 to 0.41, which corresponded to an aqueous PV of 20−24 mL. Following injection of the nonreactive tracer pulse, the column was flushed with reduced mineral salts medium for an additional 3 PVs to displace bromide. Prior to inoculation, the column flow rate was reduced to 0.0625 mL/min (50 cm/day) resulting in a hydraulic residence time of 9.5 h.

The BDI-SZ inoculum was diluted with unamended reduced mineral salts medium to yield $6.9 \pm 0.51 \times 10^5$ *Dhc* and $1.9 \pm 2.1 \times 10^5$ *Geo*SZ cells/mL. After flushing the column with one PV of reduced medium, a pulse injection of approximately 7 PVs (150 mL) of the inoculum was introduced. Similarly, in a separate set of column experiments, three PVs of reduced medium followed by approximately an 8-PV (170 mL) pulse injection of the inoculum containing $7.1 \pm 2.1 \times 10^5$ *Adehal*W cells/mL were introduced. All column experiments concluded with the introduction of five PVs of reduced medium without growth substrates. Effluent samples were collected at a frequency of four 5 mL samples per PV in 15 mL sterile centrifuge tubes using a CF-2 fraction collector (Spectrum Laboratories; Rancho Dominguez, CA). Microscopic observation of effluent samples with a Carl Zeiss Primo Star microscope (Göttingen, Germany) monitored cell breakthrough. At the termination of each column experiment, the column end plates were removed and soil was excavated in increments of 1.2 cm near the inlet (first quarter of the column) and 2.5 cm for the remainder of the column, to give a total of five segments, which were transferred into sterile 50 mL plastic centrifuge tubes. Detailed descriptions of column preparation and analytical methods are provided in the SI.

Bacterial Cell Distribution in the Aqueous and Solid Phases during Reductive Dechlorination. The distribution of nonattached and attached *Dhc* and *GeoSZ* cells was measured in similar borosilicate glass columns as above (2.5 cm diameter, 15 cm length; Kimble-Chase), but were equipped with three glass side ports to allow for aqueous phase sampling. The columns were operated at a nominal flow rate of approximately 0.04 mL/min, equivalent to a pore-water seepage velocity of 0.3 m/day and a hydraulic residence time of 1 day. The reduced mineral salts medium solution was amended with PCE and lactate. The effluent system consisted of a 20 mL glass sampling bulb to collect aqueous samples for analysis of chlorinated ethenes, ethene, pH, organic acids, and biomass. Additional aqueous samples (1−1.5 mL) were withdrawn from column sampling ports using a 2.5 mL glass syringe (Hamilton Co., Reno, NV). Columns were operated until effluent chlorinated ethene concentrations remained stable for approximately 6 PVs, and then the columns were destructively sampled to measure attached *Dhc* and *GeoSZ* cells. Each column was divided into five regions to directly compare aqueous phase and solid phase measurements; 20-g samples were collected from near the inlet, outlet and ±0.5 cm on either side of each sampling port location. Detailed descriptions of column preparation are provided in the SI.

Assessment of Microbial Surface Characteristics. To assess the influence of cell surface properties on the attachment behavior, the mean hydrodynamic diameter and electrophoretic mobility of the BDI-SZ consortium, *GeoSZ*, *AdehalW*, and the *Dhc* strains FL2, GT, and BAV1 were measured. Biomass was collected from growing (i.e., supplied electron acceptor and electron donor) and nongrowing, starved (i.e., all electron acceptor and/or electron donor were consumed) 100 mL batch cultures to mimic column experimental conditions, placed into 2 mL microcentrifuge tubes and sonicated in a water bath (Fisher Scientific; Model FS20H, 40 kHz sweep frequency) for approximately 10 min prior to dynamic light scattering (DLS) analysis. DLS analysis was performed with a Zetasizer Nano ZS analyzer (Malvern Instruments Ltd., Southborough, MA) operated in noninvasive back scattering (NIBS) mode at an angle of 173°. Approximately 1 mL of each undiluted cell suspension was loaded into a disposable cuvette (DTS0012, Malvern Instruments Ltd.) and analyzed using a green laser at a wavelength of 532 nm. All size and electrophoretic mobility measurements were performed in triplicate or more, and the operation of the analytical system was verified using a monodisperse suspension of polystyrene spheres (Nanosphere Size Standards, Duke Scientific Corp., Palo Alto, CA) with a mean diameter of 97 ± 3 nm and a zeta potential transfer standard of −68 ± 6.8 mV (Malvern Instruments Ltd.). To characterize the surface charge of aquifer materials, 10 g of Federal Fine sand and Appling soil were mixed with 20 mL of reduced mineral salt medium and sonicated for 30 min in a water bath. Immediately after 30 min of quiescent settling, the supernatants were loaded onto the Zetasizer for zeta potential analysis. The zeta potential (a measure of the magnitude of electrostatic repulsion or charge between particles or microbial cells and porous media) for different cultures and solids were calculated from the electrophoretic mobility data using the Smoluchowski equation.[47]

RESULTS AND DISCUSSION

Bacterial Cell Transport and Attachment without Supplied Growth Substrates. Following introduction of consortium BDI-SZ, *Dhc* cells and the bromide tracer were initially detected in the effluent of both the Federal Fine sand and Appling soil columns at comparable times (ca. 1 PV, Figure 1a), indicating that *Dhc* was mobile in both porous media (i.e., traveled at the same rate as the pore water) at early time (0−2 PVs). In the Federal Fine sand column, effluent *Dhc* titers increased sharply from 8×10^2 cells/mL to 1.8×10^6 cells/mL after approximately 2 PVs, and persisted at a level of 10^5−10^6 cells/mL until 7.8 PVs. Following the introduction of medium without substrates, cell titers decreased in the Federal Fine sand column, dropping below the detection limit of 10^2 cells/mL after 12 PVs (Figure 1a). Over the course of the Federal Fine column experiment, 95% of the recovered *Dhc* cells (7.1×10^7) were measured in the aqueous phase effluent, while approximately 3.5×10^6 cells (5%) were associated with the solid matrix (Table 1).

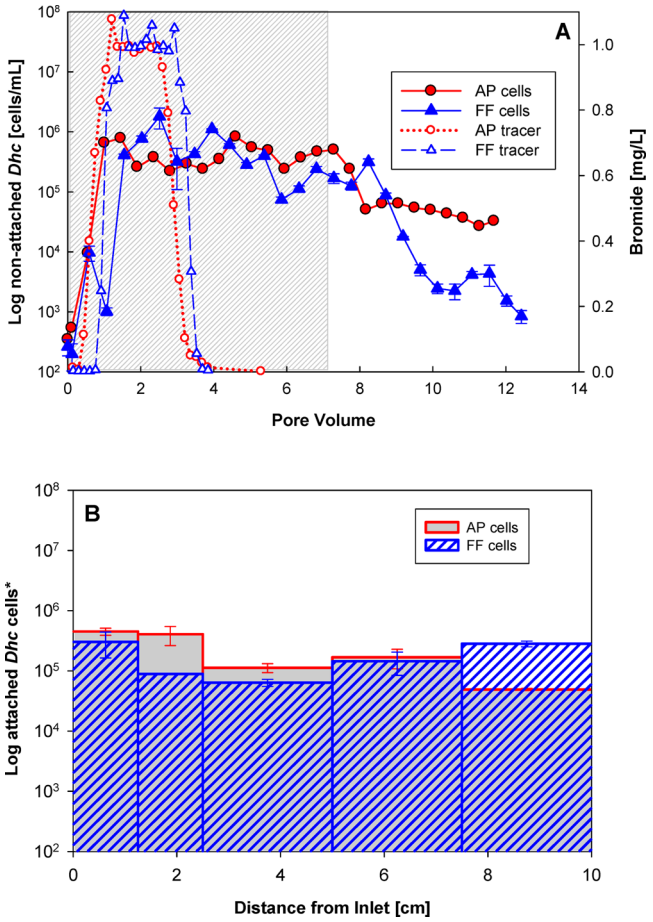

Figure 1. Distribution of (A) nonattached and (B) attached *Dehalococcoides* (*Dhc*) cells in Federal Fine Ottawa sand (FF) and Appling soil (AP) columns following delivery of inoculum in medium without supplied growth substrates. The shaded region in the upper figure denotes the duration of the inoculum pulse. *: Indicates the attached *Dhc* cells per mass porous medium with a pore volume of 1 mL (i.e., 4.98 g of AP soil and 5.54 g FF sand). All data points represent average values from triplicate samples taken from the column, and error bars represent one standard deviation. If no error bars are shown, the standard deviations were too small to be illustrated.

For the Appling soil column, effluent *Dhc* cell titers reached 9.6×10^3 per mL after 1 PV, followed by an increase to 7.8×10^5 cells/mL after 1.5 PVs, and ranged from 10^5 to 10^6 cells/

dx.doi.org/10.1021/es501320h | Environ. Sci. Technol. 2014, 48, 10878−10887

Table 1. Recovery of *Dehalococcoides* (*Dhc*), *Geobacter lovleyi* strain SZ (*Geo*SZ) and *Anaeromyxobacter dehalogenans* strain W (*Adehal*W) Cells from the Aqueous and Solid Phases Following Inoculum Delivery to Saturated Columns Packed with Federal Fine Ottawa Sand (FF) and Appling Soil (AP) without Supplied Growth Substrates[a]

	cell recovery					
	Dhc		*Geo*SZ		*Adehal*W	
	FF	AP	FF	AP	FF	AP
inoculum cells/mL ($\times 10^5$)	6.50	7.22	0.37	3.35	5.66	8.58
total cells in inoculum ($\times 10^6$)	91.5	116	5.18	53.6	118	158
aqueous phase cell recovery ($\times 10^6$)	70.9	70.7	4.88	543	43.9	115
solid phase cell recovery ($\times 10^6$)	3.49	4.55	0.0182	128	8.48	43.2
fraction of recovered cells measured as nonattached cells (%)	96	94	>99	81	84	73
total cell recovery ($\times 10^6$)	74.4	75.3	4.90	671	52.4	158
total fraction recovered (%)	81	74	95	1252[b]	52	104
k_{att} ($\times 10^{-3}$ min^{-1})	1.1	1.45	0.12	6.83	1.8	2.35

[a]FF – Federal Fine sand. AP – Appling soil. k_{att} – bacterial attachment rate coefficient. [b]Growth attributed to iron and organic matter associated with the AP soil

mL over the duration (i.e., pulse width) the consortium was injected (8 PVs). In contrast to the Federal Fine sand column, the number of *Dhc* cells eluting from Appling soil column declined more gradually following the introduction of medium, with approximately 4×10^4 cells/mL detected in the column effluent at the conclusion of the experiment (11.7 PVs, Figure 1a). The observed tailing of the *Dhc* breakthrough curve (BTC) obtained for Appling soil suggests that the cells experienced rate-limited release from the soil matrix. Despite the differences in BTCs at late time points (i.e., after 8–12 PVs), the overall number and percentage of cells recovered in the aqueous phase (7.1×10^7 cells, 94%) and retained by the solid phase (4.6×10^6 cells, 6%) were similar to those observed in the Federal Fine sand column experiments (Table 1). These findings indicate that the majority of *Dhc* cells (>94%) did not attach to the solids of both porous media examined in the absence of growth substrates.

At the termination of each experiment, the spatial distribution of cells attached to solids was determined by destructive sampling. Using the procedure outlined in Amos et al.,[11] cell numbers are reported per 4.98 and 5.54 g of saturated Appling soil or Federal Fine sand, respectively, which corresponds to the total cells (attached plus retained in pore water) present in an interrogated area containing 1 mL of pore water within the respective porous medium. The representation of cell numbers using this approach allowed for direct comparison of the total biomass in the saturated porous media to aqueous samples over the same interrogated volume of 1 mL. *Dhc* cell abundances retained with the different sections of the columns ranged from $1.8 \pm 0.5 \times 10^5$ cells per 5.45 g of saturated Federal Fine sand and $2.4 \pm 0.6 \times 10^5$ cells per 4.98 g of saturated Appling soil (Figure 1b). The spatial distribution of attached *Dhc* cells within the columns was relatively uniform over the length of each column, regardless of the porous medium.

The effluent samples from the Federal Fine columns revealed that *Geo*SZ increased in abundance from 2.7×10^2 to 7.7×10^4 cells/mL after 2 PVs, and then decreased to levels below the detection limit of 10^2 cells/mL following the introduction of medium without growth substrates (Figure 2a). Quantification

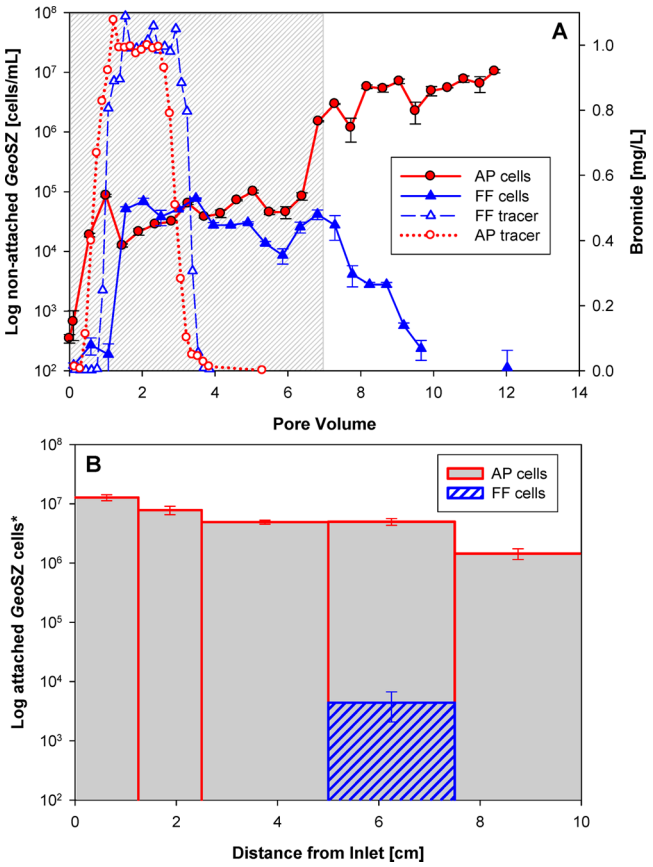

Figure 2. Distribution of (A) nonattached and (B) attached *Geobacter lovleyi* strain SZ (*Geo*SZ) cells in Federal Fine Ottawa sand (FF) and Appling soil (AP) columns following delivery of inoculum in medium without supplied growth substrates. The gray shaded region in panel A denotes the duration of the inoculum pulse. *: Indicates the attached *Geo*SZ cells per mass porous medium with a pore volume of 1 mL (i.e., 4.98 g of AP soil and 5.54 g FF sand). All data points represent average values from triplicate samples taken from the column, and error bars represent one standard deviation. If no error bars are shown, the standard deviations were too small to be illustrated.

of *Geo*SZ cells associated with the solid phase indicated that *Geo*SZ cells were not retained in the Federal Fine sand. Only one solid-phase sample, located 5–7.5 cm from the column inlet, contained *Geo*SZ cells in quantifiable numbers ($4.4 \pm 2.3 \times 10^3$ cells per 5.45 g of saturated sand) (Figure 2b). In contrast, *Geo*SZ cells were retained throughout the column at an average solid phase abundance of $6.4 \pm 0.8 \times 10^6$ cells per 4.98 g of saturated soil following the pulse injection of consortium BDI-SZ. A total of 5.4×10^8 *Geo*SZ cells (81%) were recovered in the column effluent and 1.3×10^8 cells (19%) were retained in the solid matrix (Table 1), a threefold greater fraction compared to the attached *Dhc* cells in the Appling soil column. This total cell recovery exceeded the injected number of cells by an order-of-magnitude (Table 1), indicating that growth had occurred, presumably with

dx.doi.org/10.1021/es501320h | *Environ. Sci. Technol.* 2014, 48, 10878–10887

substrates associated with the Appling soil. Prior studies have demonstrated that iron-reducing *Geobacter* spp. can oxidize and mineralize a variety of organic compounds,[48] and elemental analysis of the Appling soil indicated a total iron content of 7.2 g/kg. Despite substantially more attachment of *Geo*SZ in the Appling soil column compared to the Federal Fine sand column, cells were predominately associated with the aqueous phase in both porous media.

Similarly, *Adehal*W cells were detected in the effluent within 1 PV after the pulse injection, and reached a maximum abundance of 4−5 × 10^5 cells/mL in both Federal Fine sand and Appling soil columns (Figure 3a). Following the introduction of medium without growth substrates after eight PVs, effluent cell numbers decreased but stabilized between 2.3 × 10^4 to 6.3 × 10^5 cells/mL from PV 8 to 14.5. Retention of *Adehal*W cells by Federal Fine sand accounted for 16% (8.5 × 10^6 cells) of the recovered biomass at the conclusion of the experiment, while 84% (4.4 × 10^7 cells) were detected in the column effluent. For Appling soil, the fraction of *Adehal*W cells measured in solid phase samples was slightly higher (27%, 4.3 × 10^7 cells), with 73% (1.2 × 10^8 cells) recovered in effluent samples. *Adehal*W cells were retained over the entire length of both the Federal Fine sand and Appling soil columns, with average cell numbers of 2.5 ± 0.16 × 10^5 cells per 5.45 g of saturated sand and 1.1 ± 0.09 × 10^6 cells per 4.98 g of saturated soil, respectively (Figure 3b). Tailing was observed in the BTCs obtained for both porous media, suggesting that cells experienced rate-limited detachment, similar to what was observed for *Dhc* and *Geo*SZ in the Appling soil columns. Rate-limited detachment of *Adehal*W in the Federal Fine column led to a prolonged cell elution period at a titer of 10^5 cells/mL and incomplete cell recovery, while recovery from the Appling soil exceeded 100% and effluent titers also remained elevated (10^4 cells/mL) (Table 1). Apparently, *Adehal*W grew in the Appling soil without added substrates, presumably due to the presence of organic matter and ferric iron,[49] similar to what was observed for *Geo*SZ. Previous in situ measurements found attached *Anaeromyxobacter* cells exceeding planktonic cells by 4 orders-of-magnitude following ethanol biostimulation in a uranium contaminated aquifer,[29] suggesting that the *Anaeromyxobacter* cell distribution is strongly affected by the presence of growth substrates. Overall, the results from these bacterial transport column experiments indicate that the measured abundance of all three bacterial species examined were predominately (>70%) associated with the aqueous phase in the absence of exogenous growth substrates.

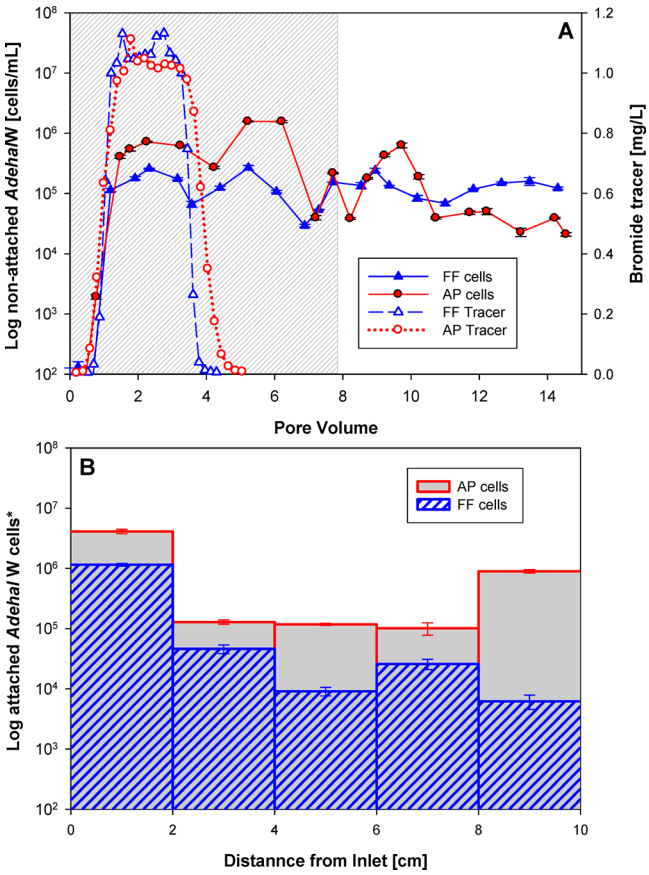

Figure 3. Distribution of (A) nonattached and (B) attached *Anaeromyxobacter dehalogenans* strain W (*Adehal*W) cells in Federal Fine Ottawa sand (FF) and Appling soil (AP) columns following delivery of inoculum in medium without supplied growth substrates. The gray shaded region in panel A denotes the duration of the inoculum pulse. *: Indicates the attached *Adehal*W cells per mass porous medium with a pore volume of 1 mL (i.e., 4.98 g of AP soil and 5.54 g FF sand). All data points represent average values from triplicate samples taken from the column, and error bars represent one standard deviation. If no error bars are shown, the standard deviations were too small to be illustrated.

Modeling Cell Breakthrough and Attachment. Microbial deposition (attachment) kinetics and cell transport within the porous media were quantified using equations that describe the processes of advection, dispersion, and deposition based on first-order attachment kinetics:[50]

$$\frac{\partial C}{\partial t} = D_H \frac{\partial^2 C}{\partial x^2} - v_p \frac{\partial C}{\partial x} - \frac{\rho_b}{\theta_w}\frac{\partial S}{\partial t} \quad (1)$$

$$\frac{\rho_b}{\theta_w}\frac{\partial S}{\partial t} = k_{att} C \quad (2)$$

where C and S are the cell numbers in the aqueous and solid phases, respectively, D_H is the hydrodynamic dispersion coefficient, x is the travel distance, t is time, θ_w is the porosity, ρ_b is the bulk density of solid, v_p is the pore-water velocity, and k_{att} is the attachment rate coefficient. D_H and θ_w were calculated from bromide tracer test experiments. Effluent BTCs and solid phase concentration profiles were simulated using these two equations, which were solved using the Hydrus-1D model version 4.14[51] with k_{att} as the fitting parameter. As illustrated in SI Figures S1−S3, the model captured the initial breakthrough of effluent bacterial cells in the column effluent, as well as the concentration plateau observed in all experiments. The fitted attachment rate coefficients (k_{att}) were consistent with the measured fraction of cells attached in the columns for all microbes tested. For example, the k_{att} values obtained in Appling soil were larger than those in Federal Fine sand, which coincided with increased bacterial retention in Appling soil (Table 1).

Bacterial transport in porous media has been traditionally simulated using models based on clean-bed filtration theory (CFT), where cells are generally considered to be inert colloidal particles. This approach is best suited for early time (initial breakthrough) since the model does not account for cell growth, death (i.e., lysis), variability in microbial cell shape and size, and changes in nutrient conditions that may impact cell

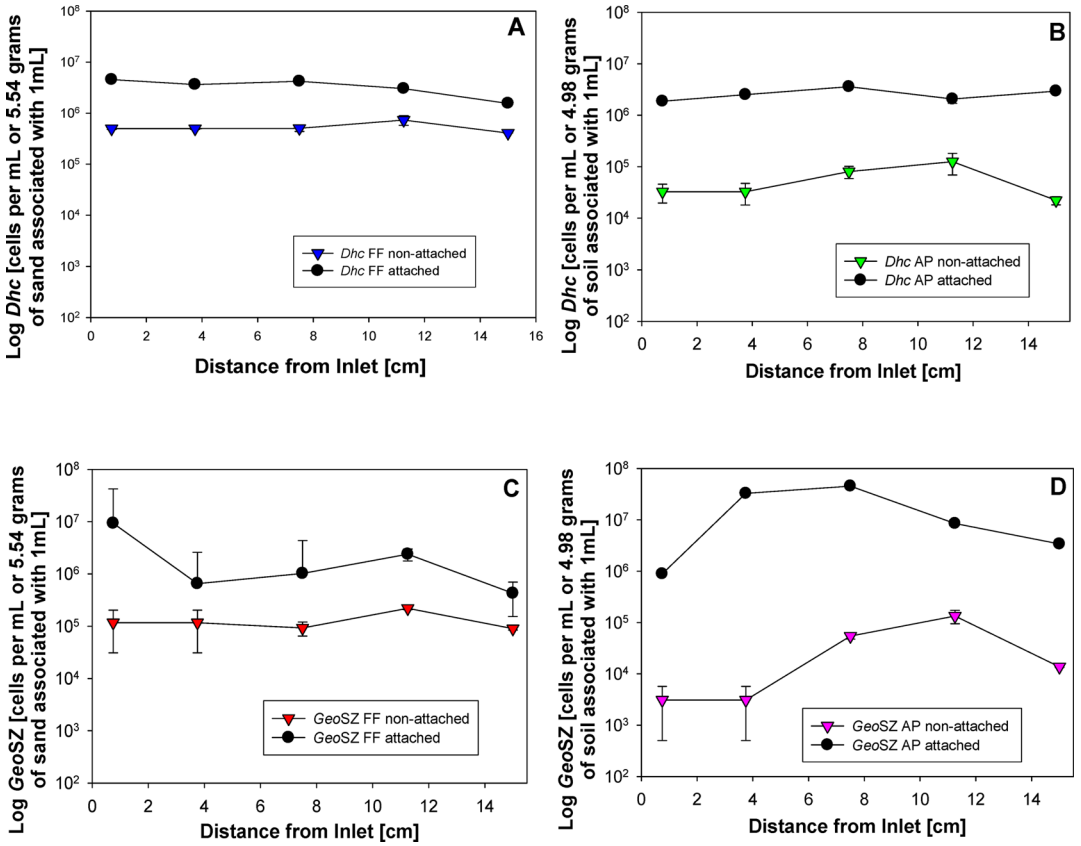

Figure 4. Distribution of nonattached and attached *Dehalococcoides (Dhc)* cells (panels A and B) and *Geobacter lovleyi* strain SZ (*GeoSZ*) cells (panels C and D) within columns packed with Federal Fine Ottawa sand (FF) and Appling soil (AP), respectively, during reductive dechlorination (0.11 mM PCE, 10 mM lactate). All data points represent average values from triplicate samples, and error bars represent one standard deviation. When error bars are not visible, they are smaller than and therefore hidden behind the data symbols. All data points represent average values from triplicate samples taken from the column, and error bars represent one standard deviation.

transport behavior over longer time scales.[7,8] Despite the limitations of the CFT model,[52,53] the model accurately captured the magnitude and rate of cell attachment observed in the experimental column studies, and thus, provides a means to estimate distribution of cells between the solid and aqueous phases during transport through water-saturated porous media. Deviations from model predictions were observed as tailing in the distal portion of the BTCs, which was likely due to cell re-entrainment (i.e., detachment or sloughing) and increased cell numbers due to cell growth at late time late time (e.g., SI Figure S2B, *Geo*SZ in Appling soil).

Bacterial Cell Distribution between the Solid and Aqueous Phases during Reductive Dechlorination. The distribution of *Dhc* and *Geo*SZ cells during active reductive dechlorination of chlorinated ethenes was quantified from colocated aqueous side-port and solid-phase samples once steady-state effluent chlorinated ethene concentrations were observed. At the termination of the experiment, influent PCE (0.11 mM) was not detected in the first sampling port (3.75 cm from the influent) or further downgradient in both the Federal Fine and Appling columns, and the reductive dechlorination daughter products *cis*-DCE, vinyl chloride and ethene were measured in the side-port samples (SI Figure S4). The effluent molar composition of *cis*-DCE, vinyl chloride and ethene was 14, 34, and 1 μM and 38, 6, and 8 μM in the Federal Fine sand and Appling soil columns, respectively (SI Figure S4). Transformation of PCE and formation of these daughter products demonstrated that *Geo*SZ and *Dhc* were active in both column systems.

Dhc cells were evenly distributed along the length of the Federal Fine sand column, with an average of $4.7 \pm 2.3 \times 10^5$ cells/mL in the aqueous phase and $3.4 \pm 1.2 \times 10^6$ cells per 5.54 g of saturated sand associated with the solid phase (Figure 4a). Similarly, *Dhc* cells were uniformly distributed over the length of the Appling soil column, with an average abundance of $7.2 \pm 4.2 \times 10^4$ cell/mL in the aqueous phase and $2.6 \pm 0.7 \times 10^6$ cells per 4.98 g of saturated soil retained on the solids (Figure 4b). Within both porous media, the numbers of cells associated with the solid phases consistently exceeded those of nonattached (i.e., aqueous phase) cells by at least a factor of 4, and by up to 2 orders-of-magnitude in the Appling soil columns.

*Geo*SZ cells revealed a different behavior and their distribution between the aqueous and solid phases ranged from nearly equal at some locations in the Federal Fine sand column to up to four orders-of-magnitude greater abundance in solids-attached cells in the Appling soil column. The average numbers of *Geo*SZ cells in the Federal Fine sand column was $1.3 \pm 0.5 \times 10^5$ cells/mL in the aqueous phase and $2.8 \pm 3.8 \times 10^6$ cells per 5.54 g of saturated sand retained in the solid phase (Figure 4c). Cell numbers in the Appling soil column averaged $4.2 \pm 5.6 \times 10^4$ cells/mL in the aqueous phase and $1.8 \pm 2.0 \times 10^7$ cells per 4.98 g of saturated soil attached to the solid phase (Figure 4d). The fraction of *Dhc* and *Geo*SZ cells measured in aqueous samples was consistently less than 2% (with one

Table 2. Percent of Nonattached *Dehalococcoides* (*Dhc*) and *Geobacter lovleyi* strain SZ (*Geo*SZ) Cells Measured in the Aqueous Phase of Federal Fine Ottawa Sand (FF) and Appling Soil (AP) Columns During PCE Reductive Dechlorination

		percent of non-attached cells			
location	distance from the Inlet (cm)	*Dhc* FF	*Dhc* AP	*Geo*SZ FF	*Geo*SZ AP
Inlet	0.75	11 ± 1.6%	1.7 ± 0.7%	1.4 ± 0.9%	0.67 ± 0.21%
Port A	3.75	14 ± 1.6%	1.3 ± 0.5%	22 ± 16%	0.02 ± 0.01%
Port B	7.5	12 ± 1.1%	2.2 ± 0.2%	12 ± 7.2%	0.14 ± 0.03%
Port C	11.25	25 ± 6.8%	12 ± 3.3%	19 ± 15%	1.91 ± 0.90%
Outlet	15.0	27 ± 8.2%	1.4 ± 0.2%	21 ± 4.1%	0.58 ± 0.36%

Table 3. Mean Hydrodynamic Diameter and Zeta Potential of Six Cultures in Medium with an Ionic Strength of 60 mM Determined Using Dynamic Light Scattering, and Interaction Energy Barriers between Bacteria and Porous Media Calculated Based on DLVO Theory in the Absence of (Non-Growth, Starving Conditions) and in the Presence of (Growth Conditions) Growth Substrates[a]

	absence of growth substrates					presence of growth substrates				
		d_H	ZP	E_{barr} (kT)			d_H	ZP	E_{barr} (kT)	
culture	cells/mL	(μm)	(mV)	FF	AP	cells/mL	(μm)	(mV)	FF	AP
BDI-SZ	1.1×10^8 (*Dhc*)/ 1.5×10^7 (*Geo*SZ)	0.96 ± 0.03	−23.0 ± 1.0	184	74.4	2.2×10^8 (*Dhc*)/ 1.9×10^7 (*Geo*SZ)	0.86 ± 0.02	−19.3 ± 1.7	123	50.1
Dhc-BAV1	5.8×10^5	2.68 ± 1.71	−22.0 ± 0.6	477	194	1.1×10^6	0.76 ± 0.07	−26.2 ± 0.7	175	70.1
Dhc-GT	2.5×10^6	1.06 ± 0.43	−32.6 ± 0.7	316	123	4.5×10^6	0.88 ± 0.05	−32.3 ± 0.9	258	101
Dhc-FL2	1.5×10^6	2.57 ± 1.28	−33.6 ± 0.9	787	304	2.8×10^6	1.39 ± 0.05	−30.5 ± 0.9	384	151
*Geo*SZ	1.7×10^7	0.84 ± 0.12	−10.5 ± 1.3	21.2	5.2	1.7×10^7	1.77 ± 0.78	−10.8 ± 0.8	15.2	−2.5
*Adehal*W	1.1×10^8	0.59 ± 0.01	−20.6 ± 1.2	94.4	38.5	1.4×10^8	0.41 ± 0.06	−12.5 ± 0.6	24.2	8.2

[a] d_H, average hydrodynamic diameter based on scattered light intensity. ZP, zeta potential based on Smoluchowski model.[47] FF, Federal Fine Sand. AP, Appling Soil. E_{barr}, Energy barrier of interactions between bacteria and porous media. The standard deviation of each sample was calculated based on at least three measurements.

exception at 12%, Table 2) in Appling soil columns. Thus, the fraction of cells recovered in aqueous samples underestimated the total (i.e., solid + aqueous phase) cells under these growth conditions. Previous studies suggested that chlorinated ethene concentrations affect cell attachment and biofilm formation.[11,12] Biofilm formation is a complicated process controlled by many environmental factors including the microbial community and contaminant concentrations, and additional studies are warranted to explore the contributions of biofilms to the reductive dechlorination process.

Assessment of Cell-Surface Interaction Energies. To further examine the influence of substrates on cell attachment, interaction energy profiles were calculated for bacterial cells and soil particles based on Derjaguin−Landau−Verwey−Overbeek (DLVO) theory, which describes the propensity for cell aggregation and the interaction forces between solid surfaces and bacterial cells (see SI). All cells were negatively charged with zeta potentials ranging from −10.5 to −33.6 mV (Table 3), which is within the general threshold range (−30 mV to +30 mV) for colloid instability,[54] indicating the tendency of the suspended cells to form aggregates (e.g., microcolonies).[55,56] In the presence of growth substrates, the zeta potential values were generally either approximately equal to or greater than the values measured in starved cultures (i.e., growth substrates consumed) (Table 3), indicating a greater propensity for attachment to the negatively charged solid surfaces.[57−59] Interaction energies between bacterial cells and Federal Fine sand grains and Appling soil particles at an ionic strength of 60 mM are summarized in Table 3 and presented in SI Figures S5A and S5B, respectively. A typical DLVO interaction energy profile of a bacterium-solid system is shown in SI Figure S5 to illustrate the primary energy barrier (peak nearest the solid surface) and a second energy minimum located approximately 7.5 nm from the solid surface. The bacterial cells may attach in the secondary energy minimum[58] or by bridging across the first energy barrier.[60]

Interaction energy profiles of all bacteria tested in the absence of growth substrates exhibited positive energy barriers and relatively shallow secondary energy minima (>−10 kT; SI Table S1). Specifically, the energy barriers of all six bacterial cultures in Federal Fine sand were more than two-times higher than those in Appling soil (Table 3), indicating that these cells are more likely to attach to Appling soil than to Federal Fine sand. With the exception of *Geo*SZ, which was nearly undetectable on the solid phase in Federal Fine sand column experiments (Figure 2B), energy barrier calculations were consistent with the relative fraction of attached cells in the column experiments without added substrates (Tables 1). For example, the energy barriers of all three *Dhc* strains in Appling soil were greater than 120 kT, which was more than twenty- and three-times higher than those calculated for *Geo*SZ and *Adehal*W, respectively (Table 3). This finding is consistent with the cells' behavior observed in the column experiments, which found that the fraction of *Dhc* cells in the aqueous phase was greater than that of *Geo*SZ and *Adehal*W cells, and that the latter were predominantly attached. In the presence of growth substrates, the primary energy barrier calculated for bacterial cells in both porous media were all lower than in the absence of substrates, indicating that the bacterial cells are more likely to attach to solids under growth conditions. The relative order of the calculated primary energy barriers was generally consistent with the experimental results, with *Geo*SZ and *Adehal*W exhibiting greater attachment to the porous media than *Dhc* strains. This theoretical analysis provides further support that characteristics of the microbe, substrate availability, and

properties of the porous media (e.g., surface charge) influence the distribution of cells between the solid and aqueous phases.

Implications for Site Assessment and Bioremediation Monitoring. Groundwater samples are typically analyzed to estimate a site's MNA or bioremediation potential; however, cell distribution between the aqueous and solid phases is a dynamic process that is controlled by a variety of organismal and environmental factors. This study demonstrated that the majority of dechlorinating cells were associated with the aqueous phase under nongrowth conditions; therefore, groundwater samples alone should be adequate to assess the abundance of key dechlorinators in oligotophic (i.e., nutrient-poor) aquifer systems. In contrast, groundwater analysis may underestimate the true cell abundance of organohalide-respiring bacteria in the aquifer by orders-of-magnitude during phases of activity (i.e., reductive dechlorination) and growth (e.g., following biostimulation with electron donor). Additionally, the column studies demonstrated that the properties of the porous medium (e.g., organic carbon content) influenced the propensity for cell attachment. For example, in Appling soil, the fraction of attached cells exceeded the planktonic cells by up to 100-fold for *Dhc* and 6,000-fold for *GeoSZ* when exogenous growth substrates were available.

Recognizing when this underestimation of *Dhc* cells in groundwater samples has implications for bioremediation practice is relevant because site management decisions are based on the abundance of *Dhc* cells in groundwater.[2,3,32] Complete dechlorination to ethene is generally observed when *Dhc* abundances in groundwater exceed 10^6 *Dhc* cells/L.[33] Therefore, when groundwater *Dhc* titers exceed 10^6 cells/L, qPCR data interpretation will not be affected and ethene formation is expected to occur regardless of the extent of *Dhc* cell abundance underestimation. Differences or variations in dechlorination rates at sites where comparable planktonic cells numbers $>10^6$ cells/L are detected may be attributed to the undetermined fraction of attached cells. At sites with intermediate *Dhc* cell abundances (i.e., 10^3–10^5 cells/L) in groundwater samples, the qPCR data interpretation in terms of reductive dechlorination potential is more challenging because the attached *Dhc* population size can vary and exceed the planktonic cell populations by several orders-of-magnitude depending on the solid matrix and electron donor availability. Similarly, the actual *Dhc* abundance at sites where *Dhc* biomarker genes are barely detected in groundwater samples may actually harbor a substantial *Dhc* population with ethene formation potential associated with the solids. Thus, failure to detect sufficient *Dhc* (i.e., $\geq 10^6$ cells/L) in groundwater may not prove that ethene formation will not occur in the aquifer formation, and additional analyses (e.g., qPCR using nucleic acids extracted from solid samples) are required to determine the aquifer's natural attenuation potential. Therefore, in aquifer formations that measure *Dhc* less than 10^6 cells/L in groundwater samples, but reductive dechlorination daughter products are present, additional analysis of aquifer solids can help to evaluate the potential for MNA or whether more aggressive treatments (e.g., biostimulation, bioaugmentation) are necessary to achieve remedial goals.

■ ASSOCIATED CONTENT

Supporting Information

Details of column preparation, sample preparation, qPCR analysis, analytical methods, DLVO calculations, calculated secondary energy minimums (Table S1), plots of mathematical modeling of bacterial breakthrough and retention (Figures S1–S3), plots of chlorinated ethene concentrations measured at the conclusions of reductive dechlorination column experiments (Figure S4) and interaction energy profile plots (Figure S5). This material is available free of charge via the Internet at http://pubs.acs.org.

■ AUTHOR INFORMATION

Corresponding Authors

*(N.L.C.) Phone: 617-627-6015; e-mail: natalie.capiro@tufts.edu.

*(F.E.L.) Phone: 865-974-4933; e-mail: frank.loeffler@utk.edu.

Notes

The authors declare no competing financial interest.

■ ACKNOWLEDGMENTS

Funding for this study was provided by the Strategic Environmental Research and Development Program (SERDP) under Project ER-1586 (contract W912HQ-07-C-0036), Project ER-2129 (contract W912HQ-11-C-0068), Project ER-2311 (contract W912HQ-13-C-0011), and Project ER-2312 (contract W912HQ-13-C-0055). The content of this manuscript has not been subject to agency review and does not necessarily represent the view of the sponsoring agency.

■ REFERENCES

(1) Lehman, R. M. Understanding of aquifer microbiology is tightly linked to sampling approaches. *Geomicrobiol. J.* **2007**, *24* (3–4), 331–341.

(2) Lu, X.; Wilson, J. T.; Kampbell, D. H. Relationship between *Dehalococcoides* DNA in ground water and rates of reductive dechlorination at field scale. *Water Res.* **2006**, *40* (16), 3131–3140.

(3) Ritalahti, K. M.; Hatt, J. K.; Petrovskis, E.; Löffler, F. E., Groundwater sampling for nucleic acid biomarker analysis. In *Handbook of Hydrocarbon and Lipid Microbiology*; Springer, 2010; pp 3407–3418.

(4) Thomas, J. M.; Lee, M. D.; Ward, C. H. Use of ground water in assessment of biodegradation potential in the subsurface. *Environ. Toxicol. Chem.* **1987**, *6* (8), 607–614.

(5) Goldscheider, N.; Hunkeler, D.; Rossi, P. Review: Microbial biocenoses in pristine aquifers and an assessment of investigative methods. *Hydrogeol. J.* **2006**, *14* (6), 926–941.

(6) Fontes, D. E.; Mills, A. L.; Hornberger, G. M.; Herman, J. S. Physical and chemical factors influencing transport of microorganisms through porous media. *Appl. Environ. Microbiol.* **1991**, *57* (9), 2473–2481.

(7) Walker, S. L.; Hill, J. E.; Redman, J. A.; Elimelech, M. Influence of growth phase on adhesion kinetics of *Escherichia coli* D21g. *Appl. Environ. Microbiol.* **2005**, *71* (6), 3093–3099.

(8) Walker, S. L.; Redman, J. A.; Elimelech, M. Influence of growth phase on bacterial deposition: Interaction mechanisms in packed-bed column and radial stagnation point flow systems. *Environ. Sci. Technol.* **2005**, *39* (17), 6405–6411.

(9) Scholl, M. A.; Mills, A. L.; Herman, J. S.; Hornberger, G. M. The influence of mineralogy and solution chemistry on the attachment of bacteria to representative aquifer materials. *J. Contam. Hydrol.* **1990**, *6* (4), 321–336.

(10) Zhang, H.; Olson, M. Effect of heavy metals on bacterial attachment in soils. *J. Environ. Eng.* **2012**, *138* (11), 1106–1113.

(11) Amos, B. K.; Suchomel, E. J.; Pennell, K. D.; Löffler, F. E. Spatial and temporal distributions of *Geobacter lovleyi* and *Dehalococcoides* spp. during bioenhanced PCE-NAPL dissolution. *Environ. Sci. Technol.* **2009**, *43* (6), 1977–1985.

(12) Schaefer, C. E.; Towne, R. M.; Vainberg, S.; McCray, J. E.; Steffan, R. J. Bioaugmentation for treatment of dense non-aqueous

phase liquid in fractured sandstone blocks. *Environ. Sci. Technol.* **2010**, *44* (13), 4958−4964.
(13) Liu, Y.; Tay, J.-H. The essential role of hydrodynamic shear force in the formation of biofilm and granular sludge. *Water Res.* **2002**, *36* (7), 1653−1665.
(14) Thomas, W. E.; Trintchina, E.; Forero, M.; Vogel, V.; Sokurenko, E. V. Bacterial adhesion to target cells enhanced by shear force. *Cell* **2002**, *109* (7), 913−923.
(15) Holm, P. E.; Nielsen, P. H.; Albrechtsen, H. J.; Christensen, T. H. Importance of unattached bacteria and bacteria attached to sediment in determining potentials for degradation of xenobiotic organic contaminants in an aerobic aquifer. *Appl. Environ. Microbiol.* **1992**, *58* (9), 3020−3026.
(16) Lehman, R. M.; Colwell, F. S.; Bala, G. A. Attached and unattached microbial communities in a simulated basalt aquifer under fracture- and porous-flow conditions. *Appl. Environ. Microbiol.* **2001**, *67* (6), 2799−2809.
(17) Pedersen, K.; Ekendahl, S. Distribution and activity of bacteria in deep granitic groundwaters of southeastern sweden. *Microb. Ecol.* **1990**, *20* (1), 37−52.
(18) Reardon, C. L.; Cummings, D. E.; Petzke, L. M.; Kinsall, B. L.; Watson, D. B.; Peyton, B. M.; Geesey, G. G. Composition and diversity of microbial communities recovered from surrogate minerals incubated in an acidic uranium-contaminated aquifer. *Appl. Environ. Microbiol.* **2004**, *70* (10), 6037−6046.
(19) Alfreider, A.; Krössbacher, M.; Psenner, R. Groundwater samples do not reflect bacterial densities and activity in subsurface systems. *Water Res.* **1997**, *31* (4), 832−840.
(20) Balkwill, D. L.; Ghiorse, W. C. Characterization of subsurface bacteria associated with two shallow aquifers in Oklahoma. *Appl. Environ. Microbiol.* **1985**, *50* (3), 580−588.
(21) Hazen, T.; Jiménez, L.; López de Victoria, G.; Fliermans, C. Comparison of bacteria from deep subsurface sediment and adjacent groundwater. *Microb. Ecol.* **1991**, *22* (1), 293−304.
(22) Haest, P. J.; Philips, J.; Springael, D.; Smolders, E. The reactive transport of trichloroethene is influenced by residence time and microbial numbers. *J. Contam. Hydrol.* **2011**, *119* (1−4), 89−98.
(23) Bekins, B.; Godsy, E.; Warren, E. Distribution of microbial physiologic types in an aquifer contaminated by crude oil. *Microb. Ecol.* **1999**, *37* (4), 263−275.
(24) Fennell, D. E.; Carroll, A. B.; Gossett, J. M.; Zinder, S. H. Assessment of indigenous reductive dechlorinating potential at a TCE-contaminated site using microcosms, polymerase chain reaction analysis, and site data. *Environ. Sci. Technol.* **2001**, *35* (9), 1830−1839.
(25) Godsy, E. M.; Goerlitz, D. F.; Grbic-Galic, D. Methanogenic biodegradation of creosote contaminants in natural and simulated ground-water ecosystems. *Groundwater* **1992**, *30* (2), 232−242.
(26) Schaefer, C. E.; Condee, C. W.; Vainberg, S.; Steffan, R. J. Bioaugmentation for chlorinated ethenes using *Dehalococcoides* sp.: Comparison between batch and column experiments. *Chemosphere* **2009**, *75* (2), 141−148.
(27) Holmes, D. E.; O'Neil, R. A.; Vrionis, H. A.; N'guessan, L. A.; Ortiz-Bernad, I.; Larrahondo, M. J.; Adams, L. A.; Ward, J. A.; Nicoll, J. S.; Nevin, K. P. Subsurface clade of *Geobacteraceae* that predominates in a diversity of Fe (III)-reducing subsurface environments. *ISME J.* **2007**, *1* (8), 663−677.
(28) Vrionis, H. A.; Anderson, R. T.; Ortiz-Bernad, I.; O'Neill, K. R.; Resch, C. T.; Peacock, A. D.; Dayvault, R.; White, D. C.; Long, P. E.; Lovley, D. R. Microbiological and geochemical heterogeneity in an in situ uranium bioremediation field site. *Appl. Environ. Microbiol.* **2005**, *71* (10), 6308−6318.
(29) Thomas, S. H.; Sanford, R. A.; Amos, B. K.; Leigh, M. B.; Cardenas, E.; Löffler, F. E. Unique ecophysiology among U(VI)-reducing bacteria as revealed by evaluation of oxygen metabolism in *Anaeromyxobacter dehalogenans* strain 2CP-C. *Appl. Environ. Microbiol.* **2010**, *76* (1), 176−183.
(30) Kerkhof, L. J.; Williams, K. H.; Long, P. E.; McGuinness, L. R. Phase preference by active, acetate-utilizing bacteria at the Rifle, CO integrated field research challenge site. *Environ. Sci. Technol.* **2011**, *45* (4), 1250−1256.
(31) Dar, S. A.; Tan, H.; Peacock, A. D.; Jaffe, P.; N'Guessan, L.; Williams, K. H.; Strycharz-Glaven, S. Spatial distribution of *Geobacteraceae* and sulfate-reducing bacteria during in situ bioremediation of uranium-contaminated groundwater. *Rem. J.* **2013**, *23* (2), 31−49.
(32) Löffler, F. E.; Ritalahti, K. M.; Zinder, S. H., *Dehalococcoides* and reductive dechlorination of chlorinated solvents. In *Bioaugmentation for Groundwater Remediation*; Springer: New York, NY, 2013; pp 39−88.
(33) Ritalahti, K. M.; Hatt, J. K.; Lugmayr, V.; Henn, K.; Petrovskis, E. A.; Ogles, D. M.; Davis, G. A.; Yeager, C. M.; Lebrón, C. A.; Löffler, F. E. Comparing on-site to off-site biomass collection for *Dehalococcoides* biomarker gene quantification to predict in situ chlorinated ethene detoxification potential. *Environ. Sci. Technol.* **2010**, *44* (13), 5127−5133.
(34) Löffler, F. E.; Yan, J.; Ritalahti, K. M.; Adrian, L.; Edwards, E. A.; Konstantinidis, K. T.; Müller, J. A.; Fullerton, H.; Zinder, S. H.; Spormann, A. M. *Dehalococcoides mccartyi* gen. nov., sp. nov., obligately organohalide-respiring anaerobic bacteria relevant to halogen cycling and bioremediation, belong to a novel bacterial class, *Dehalococcoidia* classis nov., order *Dehalococcoidales* ord. nov. and family *Dehalococcoidaceae* fam. nov., within the phylum Chloroflexi. *Int. J. Syst. Evol. Microbiol.* **2013**, *63* (Pt 2), 625−635.
(35) Sung, Y.; Fletcher, K. E.; Ritalahti, K. M.; Apkarian, R. P.; Ramos-Hernández, N.; Sanford, R. A.; Mesbah, N. M.; Löffler, F. E. *Geobacter lovleyi* sp. nov. strain SZ, a novel metal-reducing and tetrachloroethene-dechlorinating bacterium. *Appl. Environ. Microbiol.* **2006**, *72* (4), 2775−2782.
(36) Suchomel, E. J.; C.A, R.; Pennell, K. D. Evalution of trichloroethene recovery processes in heterogeneous aquifer cells flushed with biodegradable surfactants. *J. Contam. Hydrol.* **2007**, *94*, 195−214.
(37) Pennell, K. D.; Boyd, S. A.; Abriola, L. M. Surface area of soil organic matter reexamined. *Soil Sci. Soc. Am. J.* **1995**, *59* (4), 1012−1018.
(38) Wang, Y.; Li, Y.; Kim, H.; Walker, S. L.; Abriola, L. M.; Pennell, K. D. Transport and retention of fullerene nanoparticles in natural soils. *J. Environ. Qual.* **2010**, *39* (6), 1925−1933.
(39) Amos, B. K.; Suchomel, E. J.; Pennell, K. D.; Löffler, F. E. Microbial activity and distribution during enhanced contaminant dissolution from a NAPL source zone. *Water Res.* **2008**, *42*, 2963−2974.
(40) Sung, Y.; Ritalahti, K. M.; Apkarian, R. P.; Löffler, F. E. Quantitative PCR confirms purity of strain GT, a novel trichloroethene-to-ethene-respiring *Dehalococcoides* isolate. *Appl. Environ. Microbiol.* **2006**, *72* (3), 1980−1987.
(41) Amos, B. K.; Sung, Y.; Fletcher, K. E.; Gentry, T. J.; Wu, W. M.; Criddle, C. S.; Zhou, J.; Löffler, F. E. Detection and quantification of *Geobacter lovleyi* strain SZ: Implications for bioremediation at tetrachloroethene- and uranium-impacted sites. *Appl. Environ. Microbiol.* **2007**, *73* (21), 6898−6904.
(42) Ritalahti, K. M.; Amos, B. K.; Sung, Y.; Wu, Q.; Koenigsberg, S. S.; Löffler, F. E. Quantitative PCR targeting 16S rRNA and reductive dehalogenase genes simultaneously monitors multiple *Dehalococcoides* strains. *Appl. Environ. Microbiol.* **2006**, *72* (4), 2765−2774.
(43) Ritalahti, K. M.; Löffler, F. E.; Rasch, E. E.; Koenigsberg, S. S. Bioaugmentation for chlorinated ethene detoxification: Bioaugmentation and molecular diagnostics in the bioremediation of chlorinated ethene-contaminated sites. *Ind. Biotechnol.* **2005**, *1* (2), 114−118.
(44) Thomas, S. H.; Padilla-Crespo, E.; Jardine, P. M.; Sanford, R. A.; Löffler, F. E. Diversity and distribution of *Anaeromyxobacter* strains in a uranium-contaminated subsurface environment with a nonuniform groundwater flow. *Appl. Environ. Microbiol.* **2009**, *75* (11), 3679−3687.
(45) He, J.; Ritalahti, K. M.; Yang, K.-L.; Koenigsberg, S. S.; Löffler, F. E. Detoxification of vinyl chloride to ethene coupled to growth of an anaerobic bacterium. *Nature* **2003**, *424* (6944), 62−65.
(46) He, J.; Sung, Y.; Krajmalnik-Brown, R.; Ritalahti, K. M.; Löffler, F. E. Isolation and characterization of *Dehalococcoides* sp. strain FL2, a

trichloroethene (TCE)- and 1,2-dichloroethene-respiring anaerobe. *Environ. Microbiol.* **2005**, *7* (9), 1442−1450.
(47) Hiemenz, P. C.; Rajagopalan, R. *Principles of Colloid and Surface Chemistry*, 3rd ed.; Marcel Dekker, Inc.: New York, 1997.
(48) Lovley, D. R. Organic matter mineralization with the reduction of ferric iron: A review. *Geomicrobiol. J.* **1987**, *5* (3−4), 375−399.
(49) He, Q.; Sanford, R. A. Characterization of Fe (III) reduction by chlororespiring *Anaeromxyobacter dehalogenans*. *Appl. Environ. Microbiol.* **2003**, *69* (5), 2712−2718.
(50) Li, Y. S.; Wang, Y. G.; Pennell, K. D.; Abriola, L. M. Investigation of the transport and deposition of fullerene (C_{60}) nanoparticles in quartz sands under varying flow conditions. *Environ. Sci. Technol.* **2008**, *42* (19), 7174−7180.
(51) Simunek, J.; vanGenuchten, M. T.; Sejna, M. *The HYDRUS-1D Software Package for Simulating the One-Dimensional Movement of Water, Heat, And Multiple Solutes in Variable-Saturated Media*; University of California Riverside: Department of Environmental Sciences, University of California Riverside: Riverside, CA, 2008.
(52) Tufenkji, N.; Elimelech, M. Deviation from the Classical Colloid Filtration Theory in the Presence of Repulsive DLVO Interactions. *Langmuir* **2004**, *20* (25), 10818−10828.
(53) Tufenkji, N. Application of a dual deposition mode model to evaluate transport of *Escherichia coli* D21 in porous media. *Water Resour. Res.* **2006**, *42* (12), W12S11.
(54) Ma, M. The dispersive effect of sodium silicate on kaolinite particles in process water: Implications for iron-ore processing. *Clays Clay Miner.* **2011**, *59* (3), 233−239.
(55) Van Houdt, R.; Michiels, C. W. Role of bacterial cell surface structures in *Escherichia coli* biofilm formation. *Res. Microbiol.* **2005**, *156* (5−6), 626−633.
(56) Hall-Stoodley, L.; Costerton, J. W.; Stoodley, P. Bacterial biofilms: From the natural environment to infectious diseases. *Nat. Rev. Microbiol.* **2004**, *2* (2), 95−108.
(57) Walker, S. L.; Redman, J. A.; Elimelech, M. Role of cell surface lipopolysaccharides in *Escherichia coli* K12 adhesion and transport. *Langmuir* **2004**, *20* (18), 7736−7746.
(58) Redman, J. A.; Walker, S. L.; Elimelech, M. Bacterial adhesion and transport in porous media: Role of the secondary energy minimum. *Environ. Sci. Technol.* **2004**, *38* (6), 1777−1785.
(59) Tufenkji, N.; Miller, G. F.; Ryan, J. N.; Harvey, R. W.; Elimelech, M. Transport of *Cryptosporidium* oocysts in porous media: Role of straining and physicochemical filtration. *Environ. Sci. Technol.* **2004**, *38* (22), 5932−5938.
(60) Franchi, A.; O'Melia, C. R. Effects of natural organic matter and solution chemistry on the deposition and reentrainment of colloids in porous media. *Environ. Sci. Technol.* **2003**, *37* (6), 1122−1129.